

Magnetic Transitions of Superconducting Thin Films and Foils. I. Lead

G. D. CODY AND R. E. MILLER

RCA Laboratories, Princeton, New Jersey

(Received 27 February 1968)

The perpendicular and parallel magnetic transitions for pure Pb films and foils have been determined from transverse magnetization and ac susceptibility measurements as a function of thickness (400 Å to 35 μ) and temperature (1.4 to 4.2°K). The perpendicular critical field (H_{\perp}) for thicknesses less than a critical thickness, $d_c \approx 15$ kÅ, is in good agreement with the theory of Tinkham if it is assumed that the penetration depth is thickness-dependent. The data for thicknesses above d_c follow a thickness dependence predicted from the effect of a positive surface energy on the free energy of the intermediate state. At d_c there is a minimum in H_{\perp} . The parallel critical field (H_{\parallel}) up to d_c is in good agreement with the theory of Saint James and de Gennes for a second-order transition. Above d_c , H_{\parallel} agrees with the bulk value of H_{c3} for lead. In the vicinity of d_c , the magnetization curve starts to exhibit a reversible tail which persists to larger thicknesses and whose slope is in reasonable agreement with theory. From the data, the bulk values of $\kappa(T)$, $\lambda(T)$, $\lambda_L(0)$, and ξ_0 , as well as the thickness dependence of these quantities, have been computed.

I. INTRODUCTION

THE purpose of this work was to determine the thickness dependence of the transition fields of thin specimens; in particular, to examine the validity of the Tinkham-de Gennes-Saint James (TGS) theory of the transition in thin films^{1,2} and also to study the manner in which thin-film behavior is replaced by behavior characteristic of bulk specimens with positive surface energy. Experiments on Sn suggest that the thin-film-bulk transition is not continuous.^{3,4} A further purpose was to resolve the question of resistance of Pb at the magnetic transition. Published data for Sn suggest that the resistive transition occurs at fields about twice that of the magnetic transition.^{1,5}

Lead was chosen for the initial investigation chiefly for the ease of sample preparation, and also for the availability of data for $\kappa(T)$ (the Ginzburg-Landau parameter) for bulk lead.⁶ As will be seen, this quantity is the basic parameter of the theory in both the thin-film and positive surface-energy domains. Lead is an attractive material for the present investigation since it is a near-local superconductor⁷ and hence more nearly satisfies some of the assumptions of the present theories. Furthermore, while perpendicular and parallel transition measurements have been made^{3,4,8} on Sn, there do not appear to be comparable measurements for lead.

Initial results at 4.2°K have already been reported.⁹ The present paper gives a more detailed version of the experimental results and their interpretation.

II. EXPERIMENTAL PROCEDURE

A. Sample Preparation

The film specimens were evaporated onto room-temperature glass substrates (Corning 7059) at a pressure of about 8×10^{-7} mm Hg and a rate of 50 Å/sec. The magnetization samples were $\frac{7}{8}$ -in.-diam disks; strip specimens prepared in a similar manner were used for resistivity measurements. The edge of the films was scraped to remove any penumbra effects which might affect the measurements. The thickness of the films was estimated from the evaporation rate, which was determined by means of interferometric measurements as well as by room-temperature resistivity measurements. For samples greater than 50 kÅ in thickness, foils were rolled from 99.9999% lead. However, around 50 kÅ, several foil and film specimens overlapped in thickness. The thickness of each foil was determined by weighing.

B. Magnetization Measurements (Perpendicular Field)

The magnetization measurements were carried out using a conventional flux-change technique. Two pairs of identically wound sense coils were arranged such that when the sample was moved from the center of one pair of sense coils to the center of the other, an induced charge flowed which was proportional to the magnetic moment M of the sample. Each coil had 2000 turns of No. 46 copper wire wound on an average diameter of 0.6 in. The dc resistance of the four coils in series was 50 Ω at 4.2°K. The coils were wired in series with a galvanometer-galvanometer am-

¹ M. Tinkham, Phys. Rev. **129**, 2413 (1963); Rev. Mod. Phys. **36**, 268 (1964).

² D. Saint James and P. G. de Gennes, Phys. Letters **7**, 306 (1963).

³ E. Guyon, C. Caroli, and A. Martinet, J. Phys. (Paris) **25**, 683 (1964).

⁴ J. P. Burger, G. Deutscher, E. Guyon, and A. Martinet, Phys. Rev. **137**, A853 (1965).

⁵ E. H. Rhoderick, Proc. Roy. Soc. (London) **A267**, 231 (1962).

⁶ B. Rosenblum and M. Cardona, Phys. Letters **9**, 220 (1964).

⁷ J. Bardeen and J. R. Schrieffer, in *Progress in Low Temperature Physics*, edited by C. J. Gorter (North-Holland Publishing Co., Amsterdam, 1961), Vol. 3, p. 243.

⁸ R. S. Collier and R. A. Kamper, Phys. Rev. **143**, 323 (1966).

⁹ G. D. Cody and R. E. Miller, Phys. Rev. Letters **16**, 697 (1966). This work is supported by that of J. Maldy, L. Donadieu, and E. Santa-Maria, Compt. Rend. Acad. Sci. **264**, 416 (1967). 481

TABLE I. Resistivity of representative lead films at 4.2°K.

d (nominal) ^a (Å)	d (electrical) ^b (Å)	$\frac{\rho(300^\circ\text{K})^c}{\rho(4.2^\circ\text{K})}$
900	1 240	50
2 700	2 280	78
5 500	6 790	145
11 000	11 700	164
160 000	...	1600

^a From evaporation rate.^b From room-temperature resistance and $\rho(300^\circ\text{K}) = 2.1 \times 10^{-5} \Omega \text{ cm}$.^c At 4.2°K, in a field greater than H_{\perp} .

plier combination.¹⁰ The sensitivity¹¹ was determined by passing a current through a four-turn coil of known radius located between one pair of the sense coils. The external field was supplied by copper Helmholtz coils, uniform to 0.4% over the sample motion.

C. Susceptibility Measurements (Perpendicular and Parallel Field)

The complex susceptibility of the samples was measured by determining the ac impedance of one pair of the search coils with the specimen inserted and removed. The coil impedance was determined with an Anderson bridge¹² at frequencies from 100 to 10 000 cps. Typically the measuring frequency was 1000 cps, at which frequency the coils had an inductance of 150 mH and an ac resistance of 50 Ω . The applied ac field, always perpendicular to the specimen, was of the order of 0.01 G, but in several experiments was increased up to 1.0 G.

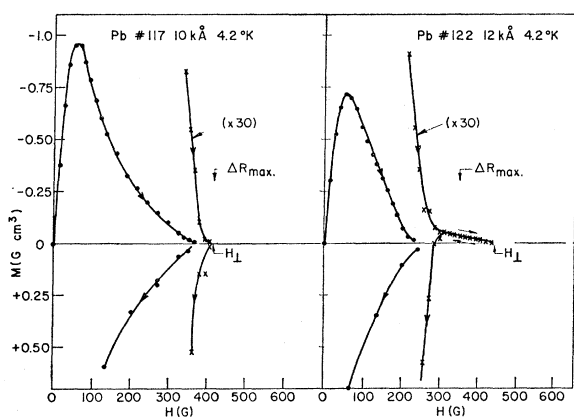


FIG. 1. Representative magnetization curves at 4.2°K. H_{\perp} denotes the magnetic transition field ($M=0$) and ΔR_{max} denotes the position of the peak in power absorption.

¹⁰ Leeds and Northrup HS2285e and Tinsley galvanometer amplifier, type 9460.

¹¹ The maximum available sensitivity, given the noise, is $7 \times 10^{-6} \text{ G cm}^3/\text{mm}$.

¹² B. I. Bleaney and B. Bleaney, *Electricity and Magnetism* (Oxford University Press, New York, 1957), p. 438.

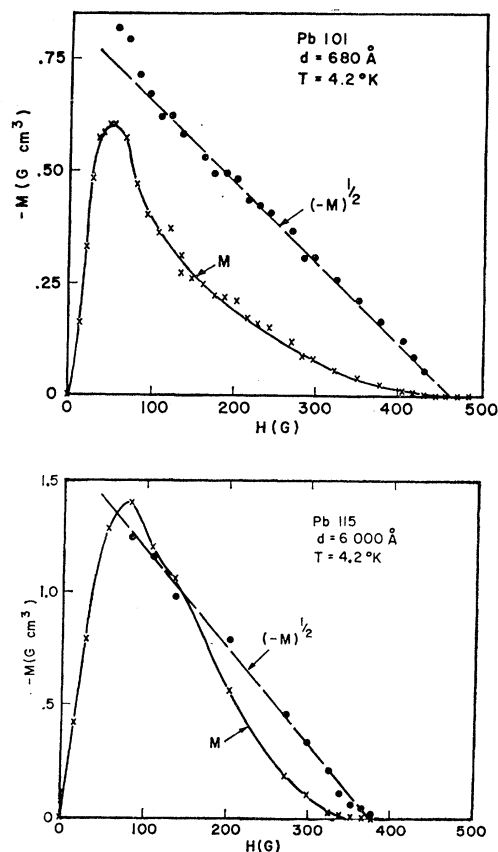


FIG. 2. (a) Magnetization curve of a 680-Å film at 4.2°K; (b) Magnetization curve of a 6000-Å film at 4.2°K.

D. Resistivity Measurements

Electrical resistivity measurements were made conventionally by a dc technique on specially prepared specimens from 900 to 10 000 Å, and one foil specimen of 160 000 Å. The purpose of the measurements was the determination of the residual resistivity ratio. Table I gives the data.

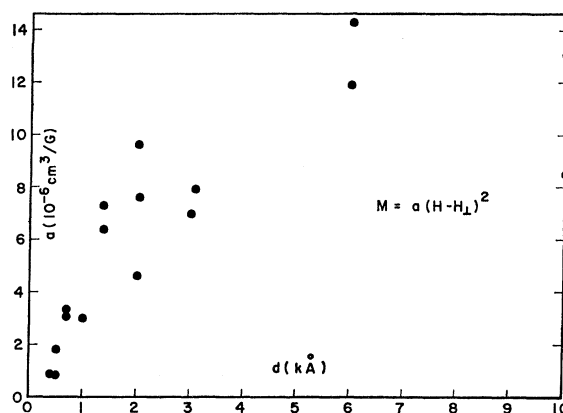


FIG. 3. The coefficient of $-M/(H-H_{\perp})^2$ as a function of film thickness at 4.2°K.

Analysis¹³ of the resistivity data in Table I leads to $\rho l = 1.5 \times 10^{-11} \Omega \text{ cm}^2$ and $l_B \approx 40 \text{ k}\text{\AA}$, where l is the mean free path and l_B is the bulk mean free path at 4.2°K . These results confirm the low-impurity content of these rapidly evaporated films.

III. EXPERIMENTAL RESULTS

Magnetization measurements in perpendicular fields were made on 27 specimens ranging in thickness from 400 \AA to $750 \text{ k}\text{\AA}$. The magnetization curves for these specimens may be divided into two distinct thickness ranges. Figures 1(a) and 1(b) show the magnetization curves for a 10 and 12-k \AA film at 4.2°K . For both thicknesses, one notes an initial perfectly diamagnetic region, a maximum moment, and then a fall-off to zero at a field H_\perp . The shape of the curve beyond the maximum for the 10-k \AA film is typical of

TABLE II. Temperature dependence of $-M/(H-H_\perp)^2 = a$.

Film	d (k \AA)	T ($^\circ\text{K}$)	a ($10^{-6} \text{ cm}^3/\text{G}$)
121	10	4.2	6.4
		3.0	3.3
		1.4	2.3
110	6	4.2	13.8
		3.0	5.8
		1.4	3.4
125	2	4.2	4.6
		3.0	2.7
		1.4	2.0
103	1.4	4.2	6.4
		3.0	3.2
		1.5	2.4
101	0.68	4.2	3.3
		3.0	2.9
		1.6	2.1

all films whose thickness d is $\lesssim 10 \text{ k}\text{\AA}$. Similarly the shape of the curve for the 12-k \AA film was typical for films and foils where $d \geq 12 \text{ k}\text{\AA}$, in particular the appearance of reversibility close to H_\perp . It appears that there is a critical thickness above which the magnetization can exhibit a reversible flux expulsion close to H_\perp . The appearance of this reversible tail depended on film thickness and temperature. The range of reversibility was reduced almost to zero, for $d \approx 12 \text{ k}\text{\AA}$ as the temperature was lowered to 1.4°K . For $d \gtrsim 15 \text{ k}\text{\AA}$, a reversible tail was observed at all temperatures.

Figure 1(a) suggests that for $d \lesssim 10 \text{ k}\text{\AA}$ the perpendicular magnetization for fields above the maximum is of the form $M \sim a(H_\perp - H)^2$. Figures 2(a) and 2(b) are indicative of the agreement of this form for M for two representative samples of the same diameter and different thickness. As will be discussed in a later section, the constant a is presumably related to the maximum critical current that can be

¹³ V. L. Newhouse, *Applied Superconductivity* (John Wiley & Sons, Inc., New York, 1964), p. 108.

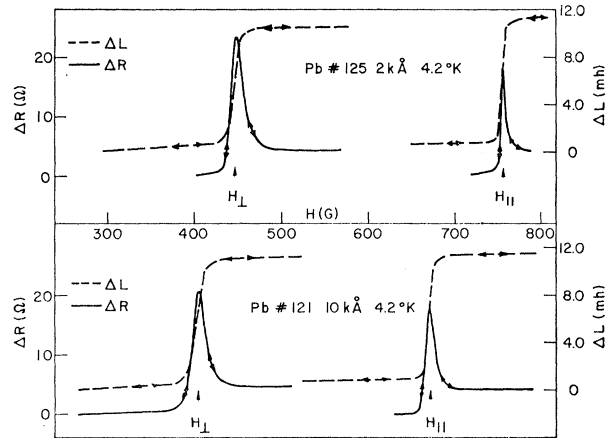


FIG. 4. Changes in the real (ΔL) and imaginary susceptibility (ΔR) of two films ($d=2 \text{ k}\text{\AA}$ and $d=10 \text{ k}\text{\AA}$) in perpendicular and parallel fields at 4.2°K .

supported by the specimen. However, its variation with thickness (Fig. 3) and temperature (Table II) is yet to be understood. It is interesting to note, however, that a similar parabolic field dependence for the critical current has been observed in type-II superconductors close to H_{c2} .¹⁴

Susceptibility data was taken on the specimens at constant frequency and amplitude as a function of the applied dc field which was either parallel or perpendicular to the plane of the specimen. The change in the real part of the susceptibility (χ') is proportional to the change in the inductance of the coil, ΔL and the change in the imaginary part of the susceptibility (χ'') is proportional to the change in the effective resistance of the coil, ΔR (see Fig. 4). Fig-

TABLE III. Comparison of susceptibility determination of $H_{||}$ with previous measurements.

d (k \AA)	T ($^\circ\text{K}$)	$H_{ }$ (G)	$H_{ }$ (G) ^a
7	4.2	640 ^b	640
4.5	4.2	670 ^b	660
	2.95	930 ^b	880
	1.45	1170 ^b	1180
2.5	4.2	760 ^b	690
	3.03	1000 ^b	960
	1.55	1270 ^b	1200
7.6	4.2	600 ^c	640
3.34	4.2	690 ^c	665
2.94	4.2	710 ^c	680
1.81	4.2	920 ^c	840
1.07	4.2	1650 ^c	1430
0.50	2.2	5500 ^d	4500

^a Interpolated from susceptibility data.

^b Thermal conductivity and electrical resistivity: T. Seidel and H. Meissner, *Phys. Rev.* **147**, 272 (1966).

^c Magnetization: see Ref. 20.

^d Thermal conductivity: D. E. Morris and M. Tinkham, *Phys. Rev.* **134**, A1154 (1964).

¹⁴ G. D. Cody and G. W. Cullen (to be published); D. B. Montgomery and W. Sampson, *Appl. Phys. Letters* **6**, 108 (1965).

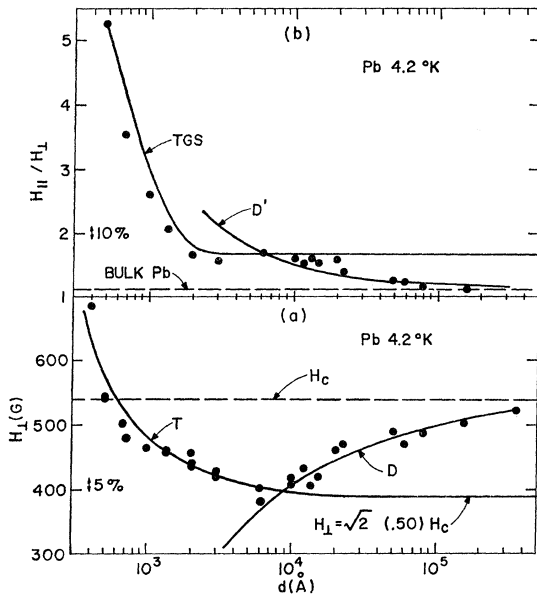


FIG. 5. (a) H_{\perp} as a function of thickness at 4.2°K; (b) H_{\parallel}/H_{\perp} as a function of thickness at 4.2°K.

ure 4 shows the results of such measurements on two films (2 and 10 kÅ) at 4.2°K and 1000 cps for parallel and perpendicular dc fields. For all specimens below 10 kÅ the peak in power absorption and the midpoint of the inductance change occurs, in a perpendicular field, at the field H_{\perp} where $M=0$. For $d \gtrsim 12$ kÅ, and again for a perpendicular field, the peak in power absorption and the midpoint of the inductance transition occurs in the reversible tail (see Fig. 1). For parallel dc fields the peak in power absorption is well within $\approx 10\%$ of the parallel transition field for lead reported in the literature. Considering uncertainties in thickness, this should be considered good agreement. A comparison of the results of the susceptibility determination of H_{\parallel} and the parallel transition fields reported in the literature is given in Table III.

The purpose of the present work was the comparison of the magnetic transition fields in the parallel and perpendicular orientation with theory. Clearly, there is no problem for the perpendicular orientation, and the field where $M=0$ (H_{\perp}) is the obvious choice for the transition field from the superconducting state. For $d \lesssim 10$ kÅ we can also use the peak in the susceptibility, but this is only a matter of convenience. For the parallel orientation the relation between the transition from the superconducting state and the measured susceptibility peak is not as clear cut, particularly when we note that for thick specimens ($d \gtrsim 12$ kÅ) in the perpendicular orientation the susceptibility peak does not coincide with the field H_{\perp} where $M=0$. However, the general agreement with previous determinations of H_{\parallel} given in Table III suggests that for $d \lesssim 7$ kÅ the identification of H_{\parallel} with the susceptibility peak is correct. Moreover, the

absence of an intermediate state for the parallel orientation, as will be seen, implies that the identification is valid over the entire thickness range.

The correlation of the peak in power absorption with either H_{\parallel} or H_{\perp} is experimentally important because the maximum of the imaginary susceptibility (χ'') is quite sharp and is considerably easier to measure than either resistivity or magnetization. Moreover, in the domain where it is utilized, both the amplitude and frequency dependence of the peak position are quite small, and hysteresis was either negligible or absent. We believe the power absorption peak is related to an intrinsic power loss in the specimen and is not due to magnetic hysteresis. A detailed discussion of this point is given in the Appendix. For the present we only state that the twofold technique of magnetization and susceptibility on the same specimen is used for the determination of H_{\perp} and H_{\parallel} .

Figures 5-7 present data taken at 4.2, 3.0, and 1.4°K and show the ratio of H_{\parallel} to H_{\perp} as a function of film thickness; the lower part shows H_{\perp} as a function of film thickness. These figures show the general trend of the data: (1) a shallow minimum in H_{\perp} that moves to larger d as the temperature is reduced; (2) for H_{\parallel}/H_{\perp} , as well as H_{\perp} , there is a rapid rise as d decreases; (3) for H_{\parallel}/H_{\perp} there is a thickness region where this ratio is about 1.6, close to the value predicted for bulk type-II superconductors; (4) for very large d the ratio approaches that observed for bulk lead^{6,15} ($H_{\parallel}/H_{\perp} \approx 1$). The curves plotted in Figs.

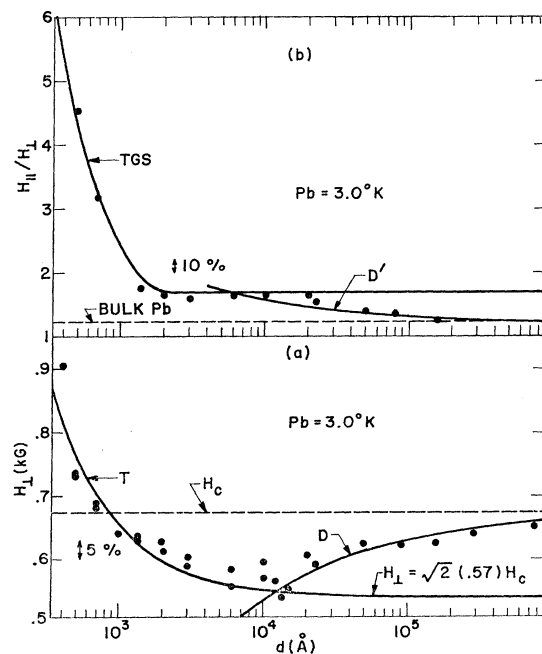


FIG. 6. (a) H_{\perp} as a function of thickness at 3.0°K; (b) H_{\parallel}/H_{\perp} as a function of thickness at 3.0°K.

¹⁵ Y. Goldstein, Phys. Letters 12, 169 (1964).

5-7 labeled by letters are theoretical, and their significance will be discussed in Sec. IV.

In addition to the above measurements at discrete temperatures, measurements of $H_{||}$ and H_{\perp} have been made on selected specimens over a continuous range. These data will also be considered in the discussion. It is worth remarking, however, that the susceptibility technique, where it is applicable, makes these measurements particularly straightforward, since it is only necessary to vary and record the field necessary to stay at the susceptibility peak as the temperature is reduced.

Finally, since questions of the order of the transition will occur in the discussion, we would like to emphasize that no field hysteresis in $H_{||}$ was ever observed. No hysteresis was observed for H_{\perp} where the points fall on the curve labeled T . For H_{\perp} data in the region where the points fall on the curve D , a field hysteresis was observed ($\approx 5\%$) for the susceptibility peak, but as noted the peak was well below H_{\perp} , and in the reversible tail. There was a suggestion of hysteresis in the magnetization curve in this region, but it is difficult to resolve it from the noise.

IV. DISCUSSION

A. Perpendicular Data: Thin-Film Region

The expected magnetic transition to the normal state for a flat-plate geometry is through the intermediate state. In this state, at the transition field, average quantities such as magnetization and specific heat vary so as to suggest a second-order transition, e.g., $M=0$, and no latent heat. However, a micro-

scopic examination of the structure of the intermediate state shows that on a fine scale the transition is of first order with a finite value of the order parameter in the initial nucleating superconducting domain.¹⁶ Tinkham pointed out that for a sufficiently thin plate the transition to the normal state might be a microscopic second-order transition with the order parameter at the transition rising continuously from zero. From Tinkham's direct calculation¹ and from the Ginzburg-Landau-Abrikosov-Gor'kov theory, one expects the transition field to be given by the following relation:

$$H_{\perp}(T, d) = \sqrt{2}\kappa(T, d)H_c(T), \quad (1)$$

where

$$\kappa(T, d) = [2\sqrt{2}\pi\lambda^2(T, d)H_c(T)]/\varphi_0. \quad (2)$$

In the above expressions $H_c(T)$ is the thermodynamic critical field, φ_0 is the flux quantum ($\varphi_0 = ch/2e = 2 \times 10^{-7}$ G cm²), and $\lambda(T, d)$ is the weak-field penetration depth which depends on the temperature and possibly on the thickness of the film. The quantity $\kappa(T, d)$ is the Ginzburg-Landau parameter which in that theory is defined only near T_c , but, in the treatment of Tinkham, is used in the above form over the entire temperature range.

If lead were a completely local superconductor, one could obtain the thickness dependence of Eq. (1) and (2) by the usual relation¹⁷

$$\lambda(T, d) = \lambda_L(T) [1 + \xi_0/L(d)]^{1/2}, \quad (3)$$

where $\lambda_L(T)$ is the London penetration depth, ξ_0 is the Pippard coherence distance, and $L(d)$ is an effective mean free path arising from either scattering by impurities or the surface of the specimen. For the present specimens with relatively long bulk mean free path, only the surface would contribute, and one expects $L \approx 8d/3$.¹⁸ However, lead is not quite local and Tinkham¹⁹ has suggested the following modification of Eq. (3) as a suitable extrapolation form for $\lambda(T, d)$:

$$\lambda(T, d) = \lambda_{\infty}(T) [1 + \lambda_L^2(T)\xi_0/\lambda_{\infty}^2(T)L(d)]^{1/2}, \quad (4)$$

which has the proper limiting behavior as $L(d)$ approaches 0 or ∞ . In Eq. (4), $\lambda_{\infty}(T)$ is the bulk weak-field penetration depth. From Eqs. (1), (2), and (4) we obtain

$$H_{\perp}(T, d) = \sqrt{2}\kappa(T, \infty)H_c(T)(1 + b/d), \quad (5)$$

where

$$\kappa(T, \infty) = 2\sqrt{2}\pi H_c(T)\lambda_{\infty}^2(T)/\varphi_0$$

and

$$b = [3\lambda_L^2(T)\xi_0/8\lambda_{\infty}^2(T)].$$

The curves labeled T in Figs. 5-7 are fitted to the form of Eq. (5), and Table IV gives the derived

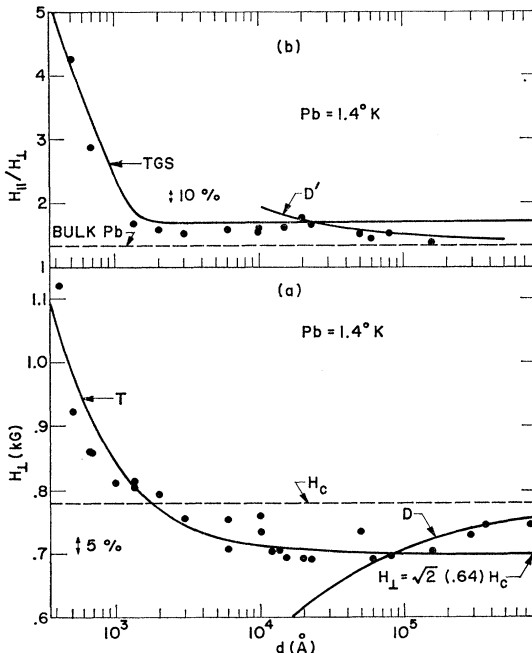


FIG. 7. (a) H_{\perp} as a function of thickness at 1.4°K; (b) $H_{||}/H_{\perp}$ as a function of thickness at 1.4°K.

¹⁶ D. S. Shoenberg, *Superconductivity* (Cambridge University Press, New York, 1962), p. 95.

¹⁷ M. Tinkham, in *Low Temperature Physics*, edited by C. DeWitt, B. Dreyfus, and P. G. de Gennes (Gordon and Breach, Science Publishers, Inc., New York, 1962), p. 166.

¹⁸ Reference 13, as pointed out by M. Tinkham.

¹⁹ M. Tinkham (private communication).

TABLE IV. Thickness and temperature dependence of $H_{\perp}(T, d)$.

T (°K)	$\kappa(T, \infty)$	b (Å)	$\kappa(T)^a$	b^b (Å)
4.2	0.50	260	0.48	200
3.0	0.57	240	0.52	200
1.4	0.64	200	0.56	200

^a From μ -wave data on bulk samples (see Ref. 6) (H_{c3} data).
^b Using $\xi_0=800$ Å, $\lambda_L(T)/\lambda \propto (T) = 0.8$ (see Ref. 7).

quantities and a comparison with independent determinations of $\kappa(T, \infty)$ and b . The agreement between the present data and previous bulk measurements is satisfactory, as is the computed and derived value of b . Furthermore, from the above analysis, and a two-fluid extrapolation [$H_c(0)=805$ G], one obtains $\lambda_{\infty}(0)=440$ Å, in fair agreement with the literature value of $\lambda_{\infty}(0)=390$ Å.²⁰

In Fig. 8, H_c/H_{\perp} is plotted as a function of T^2 for three representative films in the thickness domain where Eq. (1) is valid. For the thicker films one notes that the temperature dependence is of the form $A(1+t^2)$, in agreement with that expected from the two-fluid model ($t=T/T_c$). For the thinner film the data appear to be also linear in t^2 , but the dependence is of the form $A(1+0.7t^2)$. It is interesting to note that for the thinner film $\kappa > 1/\sqrt{2}$ over the temperature range, while for the thicker film $\kappa < 1/\sqrt{2}$.

The observed linear dependence of H_c/H_{\perp} upon T^2 was relied upon to obtain values of $\kappa(0, d)$ and $\kappa(T_c, d)$ by extrapolation. As can be seen from Fig. 8, the extrapolation to $T=0^\circ\text{K}$ is quite reliable, while that to T_c is less certain. In Fig. 9, the extrapolated values are shown plotted as a function of $1/d$. The linear dependence of κ on $1/d$ is in agreement with

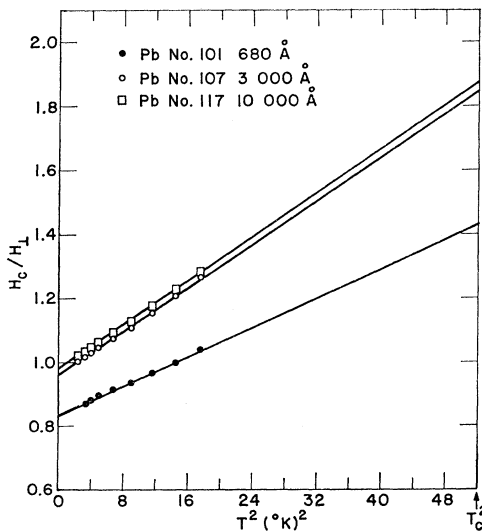


FIG. 8. H_c/H_{\perp} as a function of T^2 for several film thicknesses.

²⁰ J. M. Lock, Proc. Roy. Soc. (London) A208, 391 (1951).

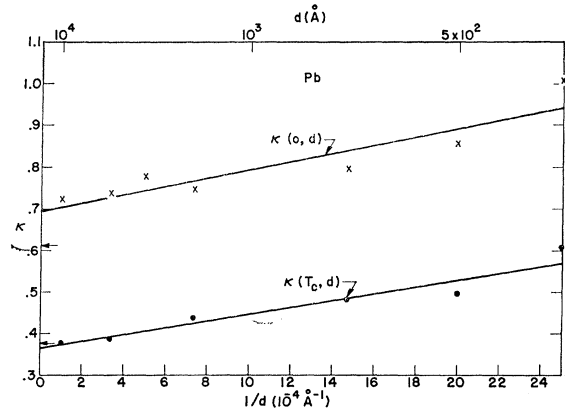


FIG. 9. $\kappa(0, d)$ and $\kappa(T_c/d)$ as a function of $1/d$. The arrows denote bulk values.

Eq. (5), as is the temperature-independent slope. The arrows indicate the bulk values obtained by Rosenblum and Cardona.⁶ One notes in Fig. 9 that as d varies from $\approx \infty$ to 500 Å, $\kappa(0)/\kappa(T_c)$ varies from 2 to 1.6.

Similar plots of $\kappa(T, d)$ against $1/d$ at temperatures of 1.4, 3.0, and 4.2°K have been utilized in preparing Fig. 10 (Table IV), which shows the temperature dependence of κ for bulk lead derived from our data. The solid curve is the expected temperature dependence for a two-fluid model for $\lambda(T)$ and $H_c(T)$ fitted to $\kappa(4.2^\circ\text{K}, \infty)$ assuming $T_c=7.2^\circ\text{K}$. The measured and extrapolated data of Rosenblum and Cardona⁶ are included for comparison.

B. Perpendicular Data: Thick-Film Region

It is clear that the Tinkham model for a second-order transition from a vortex state to the normal state can only apply where the "classical" intermediate state has a higher free energy than the vortex state. The surface energy α of a material where $\kappa < 1/\sqrt{2}$ is positive; and for thin specimens the positive surface energy of the intermediate state raise its free energy well above that of the vortex state.

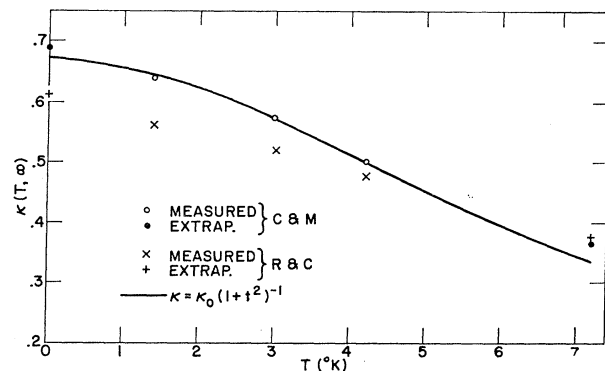


FIG. 10. $\kappa(T, \infty)$ as a function of T . The smoothed curve is based on the two-fluid model.

However, as the film thickness increases, the surface energy plays a less important role, and the intermediate state will eventually become the stable state, prior to the transition to the normal state.

In order to estimate the role of the surface-energy parameter Δ ($\alpha = \Delta H_c^2 / 8\pi$) on the transition, we consider the following simple model. Prior to the normal transition we consider an isolated superconducting domain which is assumed spherical with a diameter t . If we ignore questions of the order of the transition and consider the free energy, we obtain at the transition field H_{\perp}^D

$$H_{\perp}^D / H_c \approx 1 - \Delta / t. \quad (6)$$

Since¹⁶ $t \approx (\Delta d)^{1/2}$,

$$H_{\perp}^D / H_c \approx 1 - (\Delta / d)^{1/2}.$$

A more complicated function of (Δ / d) is obtained in the work of Davies²¹; however, the quantitative dependence upon d is similar. Recent calculations yield a coefficient of Δ / d that varies from 0.8 to 2 depending on the model.³ We can thus write more generally

$$(H_{\perp}^D / H_c) = 1 - (C\Delta / d)^{1/2}. \quad (7)$$

We can compare the transition field from Eq. (7) with that obtained from Eq. (1), in particular the critical thickness d_c , where the two are equal. From Eqs. (1) and (7),

$$d_c \approx (C\Delta) / (1 - \sqrt{2}\kappa)^2. \quad (8)$$

In Eq. (8), one can substitute values of Δ as a function of κ from the work of Bardeen ($T \approx 0^\circ\text{K}$)²² or Ginzburg ($T \approx T_c$).²³ The resultant function shows approximate symmetry about a minimum value of d_c [$d_c \approx (7-10)\lambda$ for $\kappa \approx 0.35$] and $d_c / \lambda \rightarrow \infty$ at both $\kappa \rightarrow 1/\sqrt{2}$ and $\kappa \rightarrow 0$. The rise in d_c as $\kappa \rightarrow 1/\sqrt{2}$ reflects the transition to the mixed state where $d_c \rightarrow \infty$. The rise in d_c for low κ reflects the large positive surface energy for $\kappa \rightarrow 0$, and consequent large depression of H_{\perp}^D . One can also obtain values of $d_c / 2\lambda$ from the calculations of Lasher²⁴ and Maki.²⁵ There is agreement with the simple Davies model as $\kappa \rightarrow 1/\sqrt{2}$, but large departures for low- κ material where the exact calculations imply $d_c / 2\lambda \rightarrow 0$ as $\kappa \rightarrow 0$. If the exact calculations^{24,25} are valid for low- κ material, only small thicknesses ($d_c \ll \lambda$) show a vortex transition. Since the intermediate state, with its domains, should follow the Davies curve ($d_c \gg \lambda$), it is of some interest to determine what occurs between these two limits. Unfortunately, the experimental data do not extend to low enough κ .

In Figs. 5-7, the curves labeled D are of the form of Eq. (7), and values of $C\Delta$ from 400 to 900 Å are obtained for the three temperatures. At 4.2°K, where

²¹ E. A. Davies, Proc. Roy. Soc. (London) **A255**, 407 (1960).

²² J. Bardeen, Phys. Rev. **94**, 554 (1954).

²³ V. L. Ginzburg, Physica **24**, S42 (1958).

²⁴ G. Lasher, Phys. Rev. **154**, 153 (1967).

²⁵ K. Maki, Ann. Phys. (N.Y.) **34**, 363 (1965).

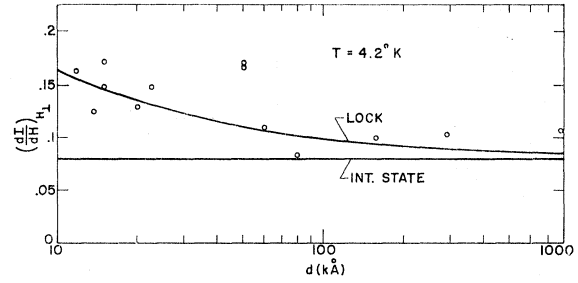


FIG. 11. The slope of the reversible magnetization curve at H_{\perp} as a function of thickness. The two curves shown are that expected for the bulk intermediate state and that derived from the effect of positive surface energy on the magnetization curve.

the precision is best, $C\Delta \approx 630$ Å, and from Bardeen²² we obtain $\Delta \approx 700$ Å, whereas from Ginzburg²³ $\Delta \approx 320$ Å ($\kappa \approx 0.5$, $\lambda \approx 470$ Å). These results maintain the factor-of-2 uncertainty in C [$C \approx 1-2$].

If the reversible tail observed in the magnetization for thick specimens ($d \gtrsim 12$ kÅ) is attributed to an intermediate state, the slope as well as the intercept is modified due to the effect of the positive surface energy. Andrew and Lock²⁶ have derived the slope of the magnetization curve of an ellipsoid in the intermediate state, to include the effect of positive surface energy and obtain

$$4\pi(1-n)(dI/dH) + 1 \approx [n - (1-n)(6.1)(\Delta/d)^{2/3}]^{-1}, \quad (9)$$

where I is the magnetization per unit volume, $4\pi n$ is the demagnetizing coefficient, Δ is the surface-energy parameter, and d is the thickness of the film, approximated by an ellipsoid. For $(1-n) \ll 1$

$$dI/dH \approx (1 + 6.1(\Delta/d)^{2/3}) / 4\pi. \quad (10)$$

In Fig. 11 the measured values of dI/dH are shown against specimen thickness. The curve through the points is a best fit of Eq. 10 with $\Delta = 730$ Å. Despite considerable scatter, there is fair agreement with the form of Eq. (10), and the value of Δ is consistent with previous estimates if $C \approx 1$.

C. Parallel Data: Thin-Film Region

In Sec. III we identified the susceptibility determination of H_{\parallel} with the parallel transition field and justified this identification by a comparison with previously reported thermal-conductivity and magnetization measurements. However, for bulk specimens there is a further ambiguity in the definition of the parallel critical field, namely the distinction between the bulk critical field (first-order transition with hysteresis) and the surface critical field H_{c3} (second-order transition without hysteresis). In general, for bulk specimens $H_{c3} = 2.4\kappa H_c$. For lead, if $T \lesssim 4.2^\circ\text{K}$ then $H_{c3} > H_c$

²⁶ E. R. Andrew and J. M. Lock, Proc. Roy. Soc. (London) **A63**, 13 (1949).

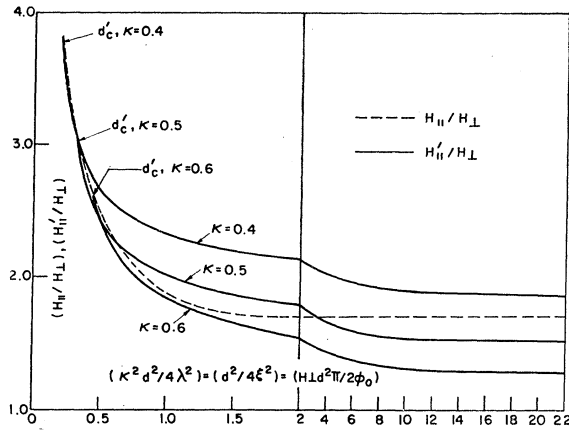


FIG. 12. A comparison of the normalized first-order field ($H_{||}'/H_{\perp}$) with the normalized second-order field ($H_{||}/H_{\perp}$) as a function of κ and $d^2/4\xi^2$.

since $\kappa > 0.42$. Between H_c and H_{c3} there exists a surface sheath which is still superconducting, and whose thickness is of the order of $\lambda(T)/\kappa(T)$. Clearly, the measured susceptibility would be expected to be sensitive to this transition and not to the ordinary transition at H_c .

For thin specimens we denote the second-order transition field corresponding to the bulk H_{c3} by $H_{||}$, and the first-order transition field corresponding to the bulk H_c by $H_{||}'$. For film thickness d such that $d < d_c' = \sqrt{5}\lambda(T)$, a second-order transition^{27,28} is expected at $H_{||}$; while for $d > d_c'$ a first-order transition should occur at the field $H_{||}'$.^{27,28} The field $H_{||}$ then represents the supercooling field.² However, for sufficiently high- κ material ($\kappa \lesssim 1/\sqrt{2}$) the field $H_{||}$ is larger than the field $H_{||}'$ for a given film thickness d , where $d > d_c'$, and can be observed experimentally. This result, similar to what occurs in bulk lead, follows from the fact that $H_{||}'$ approaches H_c in the limit where $d/\lambda \rightarrow \infty$, while $H_{||}$ approaches $2.4\kappa H_c$ in the limit where $d\kappa/\lambda \rightarrow \infty$. Thus for sufficiently large κ , and $d > d_c'$, we can have $H_{||} > H_{||}'$.

These cases are shown in Fig. 12, where $H_{||}/H_{\perp}$ and $H_{||}'/H_{\perp}$ are shown plotted against $d^2/4\xi^2 \equiv \kappa^2 d^2/4\lambda^2$. In both cases we have shown the ratio of the particular parallel critical field to the second-order perpendicular field H_{\perp} . Since $H_{||}'$ is a function of d/λ we show three curves for $\kappa = 0.4, 0.5$, and 0.6 . The first-order curves in Fig. 12 were calculated from Ginzburg and Landau²⁷ assuming $|\psi|^2$ was a constant²⁹; the second-order curve was derived from the work of Saint James and de Gennes² as given in the paper of Burger *et al.*⁴ For each of the first-order curves, the critical thickness d_c' is indicated below which the

²⁷ V. L. Ginzburg and L. D. Landau, Zh. Eksperim. i Teor. Fiz. **20**, 1064 (1950).

²⁸ D. H. Douglass, Jr., Phys. Rev. **124**, 735 (1961).

²⁹ The results of V. D. Arp, R. S. Collier, R. A. Kamper, and H. Meissner [Phys. Rev. **145**, 231 (1966)] suggest this is a reasonable approximation for finite κ .

transition is unambiguously second order. In discussing this figure we note that in an ac susceptibility experiment the transition field will be determined by the larger of $H_{||}$ and $H_{||}'$. Furthermore, if $H_{||} > H_{||}'$, the transition will be second order without hysteresis. From Fig. 12 one notes, for $\kappa \geq 0.4$, an initial second-order transition for $d < d_c'$ and a subsequent first-order transition for larger d ; for $\kappa \geq 0.5$ there is a second-order transition for $d < d_c'$, followed by a first-order transition but which for thicker films is followed by a second-order transition. For $\kappa \geq 0.6$ the transition is of second order over the entire range. In considering Fig. 12 it is important to note that as $\kappa d/\lambda \rightarrow \infty$, H_{\perp} will change from the value $\sqrt{2}\kappa H_c$ to the Davies field H_{\perp}^D , which approaches H_c . Thus, one expects the experimental curve of $H_{||}/H_{\perp}$ for $\kappa \geq 0.5$ to follow the dashed line in Fig. 12 out to the Davies region, where it will approach $1.7\sqrt{2}\kappa$.

In the upper part of Figs. 5-7, the curve marked TGS is calculated from the measured H_{\perp} , the thickness of the film d , and the function $g(d^2/4\xi^2) = g(H_{\perp} d^2 \pi / 2\phi_0)$.^{2,4} The agreement, considering the sensitivity to d for small $d/2\xi$, is good. The experimental absence of supercooling in the parallel transition reflects the above observations that for Pb in this temperature range, $H_{||} > H_{||}'$ even when $d_c > d_c'$. Furthermore, from these figures one estimates: $\xi \approx 1000$ Å and $\lambda(0.2 \text{ kA}) \approx 600$ Å. The last value compares well with $\lambda(0.2 \text{ kA}) \approx 500$ Å calculated from Eq. (4).

For film thicknesses less than d_c' , i.e., the Landau region, one expects

$$H_{||}^2(T) = [24\lambda^2(0, d)H_c^2(0)/d^2](1-t^2)/(1+t^2), \quad (11)$$

where the temperature dependence is derived assuming the usual two-fluid temperature dependence for $\lambda(T, d)$ and $H_c(T)$. In Fig. 13 we show $H_{||}^2$ as a function of $(1-t^2)/(1+t^2)$ for several films. We note that for the thinner films (500 and 680 Å) which meet the condition $d < d_c'$, the predicted linear de-

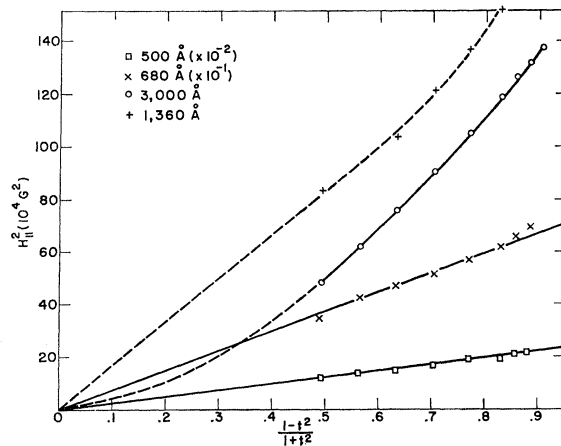


FIG. 13. $H_{||}^2$ as a function of $(1-t^2)/(1+t^2)$ for several film thicknesses.

pendence through the origin is observed. Furthermore, the observed slopes are in agreement with the slopes predicted from Eqs. (11) and (4) within 10% changes in d . The data for two thicker films (1360 and 3000 Å) have been included for comparison. The dashed portion of the curves represents a smooth extrapolation to T_c , where the limiting slope is determined by Eqs. (11) and (4), since as $T \rightarrow T_c$, $d < d_c'$ for even these films.

For films where $d > 2\xi(T) = 2\lambda(T, d)/\kappa(T, d)$, $H_{||}/H_{\perp} \approx 1.7$, and again from the two-fluid model,

$$H_{||} = 1.7[4\pi\lambda^2(0, d)H_c^2(0)/\varphi_0](1 - \beta^2)/(1 + \beta^2). \quad (12)$$

Figure (14) shows a plot of $H_{||}$ as a function of $(1 - \beta^2)/(1 + \beta^2)$ for two films of thicknesses 3 and 10 kÅ. Once again the predicted dependence is observed and the agreement of the calculated with the observed slope is excellent.

It is clear that the failure to continue the measurements to T_c subtracts somewhat from the comparison to the theory. However, the functional dependence (compare the 3000-Å sample in Figs. 13 and 14) on the temperature and the close agreement between the observed and predicted slopes gives strong support for the above interpretation. Furthermore, the absence of any observed hysteresis (supercooling) and consequent second-order transition suggests good agreement with the theory.

D. Parallel Data: Thick-Film Region

The curve D' shown in Figs. 5-7 has been calculated assuming $H_{||} = H_{c3} = 1.7\sqrt{2}\kappa H_c$. The agreement with the observed ratios is good, as can be seen from Table V, where a comparison is made between $H_{||}/H_{c\kappa}$ and its predicted value ($H_{||}/H_{c\kappa} = 2.4$). From Table V there appears to be a monotonic decrease in the ratio for the thicker foils, but the variation is small and may not be fundamental. Oxide contamination, the departure of $H_{||}$ from its limiting value, possible

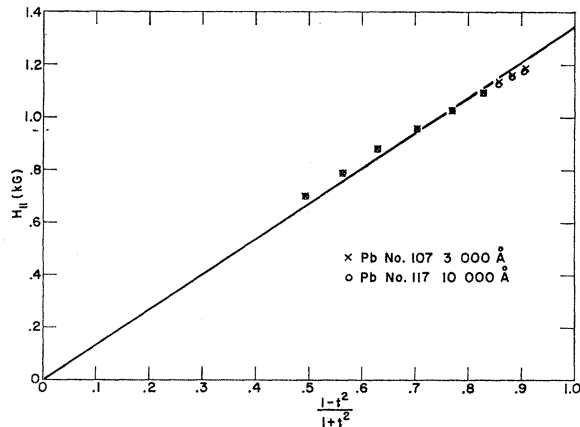


FIG. 14. $H_{||}$ as a function of $(1 - \beta^2)/(1 + \beta^2)$ for two film thicknesses.

TABLE V. $H_{||}/H_{c\kappa}$ for thick lead foils and films.

Sample	d (kÅ)	T (°K)	$H_{ }$ (G)	H_c (G) ^a	κ ^b	$H_{ }/H_{c\kappa}$
Film	50	1.4	1100	780	0.64	2.21
		3.0	873	673	0.57	2.27
		4.2	631	547	0.50	2.31
Foil	60	1.4	1002	780	0.64	2.02
		4.2	597	547	0.50	2.18
Foil	80	1.4	1045	780	0.64	2.10
		3.0	845	673	0.57	2.20
		4.2	612	547	0.50	2.23
Foil	158	1.4	983	780	0.64	1.98
		3.0	795	673	0.57	2.05
		4.2	561	540	0.50	2.05

^a Reference 16.

^b This experiment, perpendicular magnetization.

misalignment, or the effect of the ac field can play a part in the magnitude of $H_{||}$.

V. CONCLUSIONS

The present experiments, although limited to temperatures less than 4.2°K, suggest that several firm conclusions can be drawn about the magnetic behavior of thin structures of lead.

(1) In the perpendicular orientation the transition fields (H_{\perp}) were determined by magnetization. The lead films appear to obey the mixed-state relation, Eq. (1), as predicted by Tinkham,¹ up to a critical thickness d_c (≈ 10 kÅ at 4.2°K). This result has been explained by the depression of the first-order critical field far below H_c by the effects of geometry and a positive surface energy. Furthermore, in the Tinkham region, one can extrapolate from measured thin-film quantities to bulk values and the agreement is very good. Similar agreement for In and Sn was found by Chang and Serin although the analysis was somewhat different.³⁰

(2) In the parallel orientation, transition fields were determined by a susceptibility technique. There is good agreement between the measured fields and those given by the second-order transition predicted by de Gennes and Saint James up to a thickness of the order of d_c . In this range $H_{||} = H_{\perp}g(H_{\perp}d^2\pi/2\varphi_0)$, where g is a known function. In the limit $d \rightarrow 0$ one obtains $H_{||} \cong (\sqrt{24})\lambda H_c/d \approx (\sqrt{24})\lambda_L(T)\xi_0^{1/2}H_c(T)/d^{3/2}$. In the domain $2\xi \lesssim d \lesssim d_c$, one obtains the type-II result $H_{||} \approx 1.7H_{\perp}$, but where $\kappa < 1/\sqrt{2}$. This result suggests a considerably wider thickness range for the second-order transition than had been supposed. These results can be explained in terms of the high values of κ observed for lead in this temperature range.

(3) Above d_c , H_{\perp} follows an expression of the form predicted by considerations of the effect of positive surface energy on the transition. $H_{||}$, on the other hand, is in fair agreement with the value predicted for the field $H_{c3} = 2.4\kappa H_c$.

³⁰ G. K. Chang and B. Serin, Phys. Rev. **145**, 274 (1966).

(4) The shape of the magnetization curve prior to the transition field H_{\perp} is consistent with the above observations. For thicknesses less than d_c the magnetization is irreversible and away from the Meissner region is of the form $M = \pm a(H - H_{\perp})^2$. For thicknesses above d_c , the magnetization close to H_{\perp} is reversible and linear, with a slope in fair agreement with that calculated from theories of the intermediate state as modified by positive surface energy.

(5) Low-frequency susceptibility measurements have proved to be a useful tool for determining H_{\perp} for $d < d_c$ and H_{\parallel} over the entire range of thickness. The detailed discussion in the Appendix associates the peak in power absorption observed as a function of field with an eddy-current mechanism where a similar peak is observed as a function of frequency. At the superconducting transition there is a transition from $\rho^* = 0$, characteristic of the superconducting state, to $\rho^* = \rho_N$, characteristic of the normal state. If the thickness of the foil or film satisfies an optimum coupling condition a peak will occur. This model has been shown to satisfactorily explain the observed data. Consistent with the model is the fact that the peak in power absorption occurs in the reversible tail of the magnetization curve for thick specimens. Further verification is seen from the observation that the peak disappears for very thick specimens for the range of frequencies employed.

(6) As noted in the Appendix, it appears that low-frequency susceptibility measurements should prove useful in determining the normal resistivity of high-purity thin foils. In the absence of a solution to the complex boundary value problem, an empirical expression for the occurrence of a resistive peak was obtained as a function of frequency, radius, and thickness.

(7) Finally, it is important to emphasize the power of magnetic transition measurements in parallel and perpendicular fields on the *same specimen*. In terms of the present theory one can determine from these data $\lambda(T, d)$, Δ , $\kappa(T, d)$, $\lambda_L(0)$, and ξ_0 , as well as the thickness of the film.

We plan to continue the lead measurements, particularly for thin films, to T_c , where the transition from κ less than $1/\sqrt{2}$ to greater than $1/\sqrt{2}$ should occur as a function of temperature. Measurements on tin are discussed in a subsequent paper.³¹

ACKNOWLEDGMENTS

We are grateful to J. Gittleman for numerous discussions and to G. Weisbarth for preparation of the film specimens.

APPENDIX: SUSCEPTIBILITY MEASUREMENTS OF THIN FILMS IN THE NORMAL AND SUPERCONDUCTING STATE

In the present paper the peak in the effective resistance of the specimen coil has been used as a con-

³¹R. E. Miller and G. D. Cody, following paper, Phys. Rev. **173**, 494 (1968).

venient probe (along with the magnetization) for H_{\perp} for $d \leq 10$ kÅ and to define H_{\parallel} for $450 \text{ Å} \leq d \leq 160$ kÅ. Where comparisons can be made, the value of H_{\parallel} defined in this manner agrees with existing data for the parallel field. However, the source of the resistance peak has yet to be explained, as well as its behavior under changes in frequency (f), amplitude of ac field (h), and radius of sample (r). The majority of the data points were taken at $f = 1000$ cps and $h \approx 0.01$ G; however, for selected specimens, frequencies from 100 cps to 10 kcps and ac fields up to 1 G were used. In the course of this examination several experimental observations were noted. These observations are listed below and cover the following phenomena:

(1) The magnitude of the resistance peak $(\Delta R)_{\max}$ where ΔR is the difference between the effective resistance of the coil when the sample is inserted and when it is removed. For *parallel* and *perpendicular* orientations we find $(\Delta R/f)_{\max} = (0.18 \pm 0.04)r^3 \Omega/\text{cps}$.

(2) The frequency dependence of the field H_p where the resistance peak occurs. For the two orientations we find (a) in perpendicular fields:

$$d \lesssim 10 \text{ kÅ}, (dH_p/df)_{\perp} = 0;$$

$$d \gtrsim 12 \text{ kÅ}, (dH_p/df)_{\perp} = \text{const};$$

(b) in parallel fields: $d \lesssim 10$ kÅ, $(dH_p/df)_{\parallel} = 0$;

$$d \gtrsim 12 \text{ kÅ}, (dH_p/df)_{\parallel} \lesssim 0.1 (dH_p/df)_{\perp}.$$

(3) The dependence of the field H_p on the ac amplitude (h). For the two orientations we find $(H^* - H_p) = Kh^{1/2}$, where (a) in perpendicular fields: $d \lesssim 10$ kÅ, $H^* = H_{\perp}$; $d \gtrsim 12$ kÅ, $H^* < H_{\perp}$ (i.e., in the reversible tail); (b) in parallel fields: $K_{\parallel} \approx 0.1K_{\perp}$ and $H^* = H_{\parallel}$.

(4) The total inductance change at the transition. We find that the inductance change ΔL in both parallel and perpendicular fields satisfies the relation $(\Delta R)_{\max} = 0.32\Delta L(2\pi f)$. Furthermore, H_p corresponds closely to the field where the inductance has changed by one-half its maximum shift.

(5) The disappearance of the power absorption peak for thicker films. For films $\gtrsim 160$ kÅ and for the frequencies $\gtrsim 600$ cps the power-loss peak disappears for both the parallel and perpendicular orientations.

(6) The existence of harmonic generation at the peak position. We find appreciable odd harmonic (chiefly third) at the peak position.

It should be emphasized that the frequency and amplitude dependence of H_{\perp} or H_{\parallel} [observations (2) and (3)] is a very small effect. At the frequency and ac field used any uncertainty in H_{\perp} or H_{\parallel} due to this cause was well below 5%. However, any satisfactory theory should be able to explain all of the above observations.

Magnetic hysteresis, as discussed by Bean,³² is

³²Charles P. Bean, Rev. Mod. Phys. **36**, 31 (1964).

a qualitative explanation of the above characteristics. However, although many of the above features can be understood in terms of such a hysteresis model, there are several objections. A hysteresis model would not readily explain the numerical agreement between the loss observed for the same specimen in parallel and perpendicular orientations. Furthermore, the appearance of the loss peak in the reversible portion of the magnetization curve (perpendicular field, $d > 12$ kÅ) would be surprising on a hysteresis model. Moreover, the frequency dependence of the peak position for $d \gtrsim 12$ kÅ again does not suggest hysteresis. Finally the model does not explain the disappearance of the peak in power absorption as the frequency is raised for thick films (≈ 160 kÅ). Fortunately, there is an alternative explanation that can explain *all* of the above observations, with a minimum of assumptions. The success of this model, an eddy-current model, suggests that hysteresis plays a relatively minor role. Before discussing this model, as applied to the superconducting transition, it is necessary to consider eddy-current power absorption in normal foils and films.

Eddy-Current Power Absorption in the Normal State

In the literature there are numerous calculations of the complex impedance of conducting cylinders and spheres in uniform ac fields.³³ The general result is that at low frequencies the loss per cycle ($\Delta R/f$) is low because, despite the almost complete penetration, the driving force dh/dt is low. At high frequencies, the loss is also low, despite the large dh/dt , since the field only extends a skin depth into the material. These general observations suggest a maximum, and analysis shows that for an infinite cylinder of radius r parallel to h the maximum loss per cycle occurs when $r/\delta = 1.8$. The quantity r is the cylinder radius (cm), δ is the skin depth given by $\delta = (10^9 \rho / 4\pi^2 f)^{1/2}$, and ρ is the resistivity, in Ω cm. At the maximum, $(\Delta R/f)_{\max}$ can easily be shown to be

$$(\Delta R/f)_{\max} = (\pi r^2 d) (0.19 \times 10^{-7}) (h/I)^2, \quad (\text{A1})$$

where d is the length (cm) of the "infinite" cylinder

TABLE VI. Copper foil characteristics.

Sample	r (cm)	d (10^{-3} cm)	ρ_{dc} (10^{-8} Ω cm) ^a	f_{\max} (cps) ^b	$(\Delta R/f)_{\max}$ (10^{-2} Ω /cps)
C1	0.475	2.54	0.805	450	2.21
C2	0.635	1.02	1.74	2000	4.41
C3	0.635	0.74	2.14	4000	4.61
C4	0.475	1.32	1.08	1500	1.95
C5	0.635	1.32	1.08	850	4.45
C6	0.635	1.32	1.08	900	4.72
C7	0.635	2.54	0.805	300	4.86

^a Directly measured.

^b Frequency where maximum in $(\Delta R/f)$ occurs.

³³ Cf. L. D. Landau and E. M. Lifshitz, *Electrodynamics of Continuous Media* (Pergamon Press, Inc., New York, 1960), p. 186.

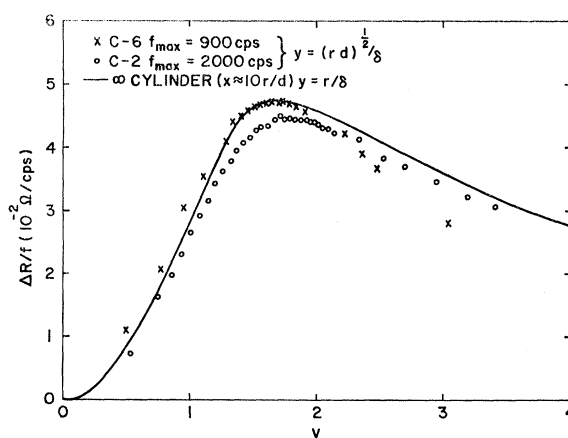


FIG. 15. The increase in the ac resistance of a coil for two thicknesses and radii of copper as a function of $(rd)^{1/2}/\delta$. For comparison the normalized ac resistance for an infinite rod is shown as a function of r/δ .

and I is the current in amps in the external coil supplying the field h (gauss). In the present experiment $h/I = 2.34 \times 10^3$ G/A and hence

$$(\Delta R/f)_{\max} = (0.33) r^2 d \Omega/\text{cps}. \quad (\text{A2})$$

This value for $(\Delta R/f)_{\max}$ is smaller than the experimental result [observation (1)] by a factor of order r/d .

The factor r/d strongly suggests demagnetizing effects due to the flat-disk geometry. Unfortunately, there does not appear to be an exact calculation on eddy-current losses in disklike ellipsoids. In the absence of such, we have examined copper disks whose characteristics are given in Table VI.³⁴ We find that a maximum in $\Delta R/f$ occurs when $(rd)^{1/2}/\delta \approx 1.8$, and at the maximum

$$(\Delta R/f) = (0.18) r^3, \quad (\text{A3})$$

which is in good agreement with the maximum loss observed at the fields H_{\perp} and H_{\parallel} for the lead films and foils. For the copper foil in the normal state, the enhancement of $(\Delta R/f)_{\max}$ by (A3) over that given by Eq. (A2) is of the order of 100. For a 500-Å Pb film, however, the enhancement would be of the order of 50 000. Figure 15 shows $\Delta R/f$ for two copper foils as a function of $(rd)^{1/2}/\delta$. For comparison we also show the computed loss per cycle for an infinite cylinder (enhanced by $10r/d$) as a function of r/δ .³³ The shape of the curves appears to be similar.

The occurrence of the peak in $\Delta R/f$ at $(rd)^{1/2}/\delta \approx 1.8$ is a plausible result from dimensional considerations alone, and the enhancement of the loss by the factor r/d is a characteristic of demagnetizing effects in a disk geometry. At the maximum in power loss, the real susceptibility of the disk is of the order of $(-r/8\pi d)$, and there is an appreciable buildup of the

³⁴ In Ref. 9 we reported $d/\delta \approx 0.1$; however, magnetoresistive effects and failure to change the radius obscured the result. For the lead samples $(R/d)^{1/2} \approx 20$.

applied field h at the edge. A rough calculation of demagnetizing effects on eddy currents for ellipsoids leads to a loss maximum of

$$(\Delta R/f)_{\max} \approx 0.2r^3,$$

in agreement with Eq. (A3), but the peak in this calculation occurs at $d/\delta \approx 1.8$, which differs by a factor $(r/d)^{1/2} \approx 15$ from the peak position observed for the copper foils.

In the following section, we apply the results empirically obtained for normal copper disks as a function of frequency to the peak observed in ΔR for superconducting lead, as a function of H . In essence, we propose that the large variation in resistivity at the superconducting-to-normal transition has the same effect on $(rd)^{1/2}/\delta$ as the variation of frequency employed for the normal copper disks.

Low-Frequency Losses of Superconducting Disks at H_{\perp} and H_{\parallel}

The eddy-current model clearly satisfies observation (1) and explains the absence of a thickness dependence on the maximum loss. Furthermore the fact that for both cylinders and spheres³³ $\Delta R_{\max} \approx 0.4\Delta L_{\max}(2\pi f)$ suggests that observation (4) is to be expected. Two additional assumptions are required for observations (2) and (3), namely the existence of a critical current (I_c) against flux penetration for the film and foil, and a resistive mechanism (ρ^*) for power loss once flux penetrates. The first assumption, a critical current, can be justified by considering either a fundamental current density for the material³⁵ or by the concept of flux pinning and a critical Lorentz force.³⁶ The second assumption, an effective resistivity ρ^* when flux penetrates, can be justified from the numerous results obtained on flux-flow resistivity in the mixed state.³⁷ The maximum value of ρ^* will be ρ_N (the normal resistance) but at the transition field ρ^* could be considerably less than ρ_N . The following sections consider the consequences of these assumptions.

The magnetization data for the films (Table II) and recent experiments on type-II materials¹⁴ suggest the following form for the critical current I_c : $I_c = B(H - H^*)^2$, where B is a constant which is a function of the radius and thickness of the disk. The quantity H^* is the critical field for the current. One would normally expect $H_{\perp}^* = H_{\perp}$ and $H_{\parallel}^* = H_{\parallel}$. However, in the case of an intermediate state, with reversible flux distributions, one might expect $H_{\perp}^* < H_{\perp}$.

Consider a superconducting disk in the ac field h . If the disk can shield itself from the applied field, with a current less than I_c , no flux will enter and

there will be no change observed in either the real or imaginary susceptibility. If the induced current required for perfect shielding is larger than I_c , flux will enter and a power dissipating mechanism is available due to flux flow. If $2\pi(dr/10^9\rho_N)^{1/2} < 1.8$, we will observe a peak in the power absorption as the effective resistivity of the disk sweeps, as a function of field, from $\rho^* = 0$, characteristic of the superconducting state, to its maximum value $\rho^* = \rho_N$, characteristic of the normal state. Furthermore, the maximum loss per cycle as a function of field will again be given by the eddy-current result, Eq. (A3).

For this model we can calculate the shift in peak position H_p with ac field h for the perpendicular orientation. At the peak in power absorption the induced current can be estimated as $I \approx \frac{1}{2}hr$, where h is in gauss, r in cm, and I in amps. From the magnetization data (Table II) we estimate for $d \approx 6$ kÅ, $B \approx 150 \times 10^{-6}$ A/G² and for $d \approx 15$ kÅ, $B \lesssim 80 \times 10^{-6}$ A/G². By equating the induced current to I_c we obtain

$$H^* - H_p = Kh^{1/2} = (r/2B)^{1/2}h^{1/2}. \quad (\text{A4})$$

For $d = 6$ kÅ, $r = 0.5$ cm, we calculate $K \approx 40$ G^{1/2} and we observe $K \approx 60$ G^{1/2}. For $d = 15$ kÅ, $r = 0.39$ cm, we calculate $K \gtrsim 50$ G^{1/2} and we observe $K \approx 90$ G^{1/2}. The agreement appears satisfactory.

For films where $d \lesssim 10$ kÅ, $H_{\perp}^* \approx H_{\perp}$, which implies either perfect pinning or a critical current that vanishes at H_{\perp} . For films where $d \gtrsim 12$ kÅ,

$$H_{\perp}^* < H_{\perp} (H_{\perp}^* \approx 0.8H_{\perp}).$$

This result is unexplained, but agrees with the observation that reversibility occurs above ≈ 12 kÅ. Clearly, if flux can be pinned, the adjustment of normal and superconducting domains required to give a reversible magnetization will not occur. It is interesting to note the clear departure from the Bean³² model at this point. Power losses occur in this model at a field less than H_{\perp} , due to the reversibility of the dc magnetization curve.

We can also calculate the frequency dependence of the peak position for the perpendicular case from the present model. For $d \lesssim 10$ kÅ where $H_{\perp}^* \approx H_{\perp}$, we do not expect the peak position to depend on frequency [observation 2(a)] because of the rapid rise in resistance over an interval $(dH_{\perp}/dT)\Delta T_c$, where ΔT_c is the width of the zero-field transition. For $d \gtrsim 12$ kÅ, where $H_{\perp}^* < H_{\perp}$, one expects a gradual rise in resistance. Indeed, if ρ^* is the effective resistivity that satisfied the skin-depth condition

$$\rho^* = (4\pi^2 f r d) / (1.8)^2 \times 10^9, \quad (\text{A5})$$

and if $\rho^* = \rho^*(H)$,

$$(df/dH_p) = (0.82 \times 10^8 \rho_N / H_{\perp} r d), \quad (\text{A6})$$

where H_p is the field at which the peak occurs at a given frequency f , and we have assumed the flux-flow result $d\rho^*/dH_p = \rho_N/H_{\perp}$.³⁷

³⁵ John Bardeen, Rev. Mod. Phys. **34**, 667 (1962).

³⁶ P. W. Anderson and Y. B. Kim, Rev. Mod. Phys. **36**, 39 (1964).

³⁷ Y. B. Kim, C. F. Hempstead, and A. R. Strnad, Phys. Rev. **139**, A1163 (1965).

TABLE VII. Effect of frequency on peak position.

Film	d (10^{-4} cm)	r (cm)	df/dH_p (cps/G)	ρ^* (Ω cm) ^a	H_{\perp} (G)	ρ_N (10^{-8} Ω cm) ^b	ρ_{dc} (Ω cm) ^c
120	1.5	0.38	220	7×10^{-10}	445	7	1×10^{-7}
19	6	0.60	22	4.4×10^{-9}	470	3	2×10^{-8}
6	16	0.60	5.6	1.2×10^{-8}	496	2	1.3×10^{-8}

^a At 1000 cps from Eq. (A5).^b From Eq. (A6).^c Measured directly.

We have observed a linear shift in peak position with frequency for $d \geq 12$ kÅ [observation 2(a)] and Table VII summarizes the experimental results for the dependence of peak position on frequency for the case where $H_{\perp}^* < H_{\perp}$. The last two columns compare the computed ρ_N from the flux-flow resistance with the measured dc resistance. The agreement, within a factor of 2, is satisfactory, considering the almost two orders of magnitude variation in df/dH_p . It would be very difficult to account for these data in terms of a hysteresis model.

For the parallel orientation the low values of K and dH_p/df can be explained by the absence of an intermediate state. Furthermore, the induced current is orthogonal to the magnetization current and the flux-flow resistivity is quite low because of the absence of a dc perpendicular field. For the same reasons we would expect $H_{\parallel}^* \approx H_{\parallel}$. However, increasing ac amplitude does change the angle of the field with the surface of the specimen and this may also play a role.¹

Further confirmation for the present model can be seen when one examines the condition for the appearance of a maximum in the resistivity upon making the transition to the normal state. If expressed in terms of frequency for a given ρ_N , d , and r , the condition is

$$f < (\rho_N / 1.22 \times 10^{-8} r d).$$

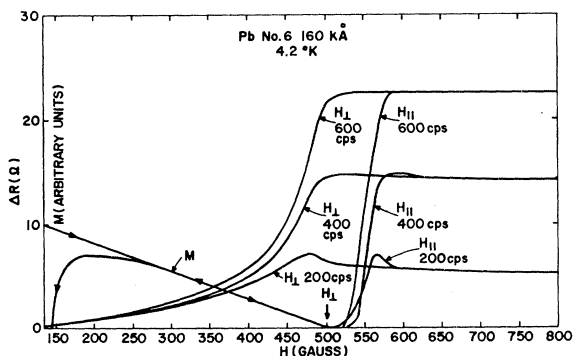


FIG. 16. Magnetization and ΔR as a function of field and frequency for a foil of lead at 4.2°K (160 kÅ).

However, if we observe a peak in the *normal* state in $\Delta R/f$, as a function of frequency, at a frequency f_0 we have

$$f_0 = (\rho_N / 1.22 \times 10^{-8} r d).$$

Thus, if $f < f_0$ one expects to see a peak as a function of field in the superconducting state; if $f > f_0$ no peak should be observable. For a 160-kÅ Pb foil in the normal state we observed the frequency-dependent peak at 450 cps. As Fig. 16 shows, no peak at the magnetic transition from the superconducting state was observed as a function of field at 600 cps, but appeared at 400 cps for both parallel and perpendicular transitions.

The above discussion has covered observations (1)–(5). Observations (6), which is at first suggestive of a hysteresis mechanism, is also in the present model since the resistivity that occurs in the eddy-current equation is clearly nonlinear. Unfortunately, the mathematical problem of solving the differential equations for the present geometry is such that nonlinear effects can hardly be considered in detail.

In the present discussion we have emphasized an alternative model to the usual hysteresis model, both to understand a variety of phenomena but also to emphasize the usefulness of the technique to measure the very low resistances that occur in the intermediate state or at the transition fields H_{\perp} and H_{\parallel} . A measure of the sensitivity can be given when it is realized that at 100 cps a peak occurs for a 500-Å film 1 cm in diameter when $\rho^* \approx 3 \times 10^{-12}$ Ω cm. Of course it must be realized that the induced current density is not negligible, being of the order h/d (for a 500-Å film the induced current is of the order of 2×10^8 A/cm²).

In the present measurements the technique was applied for H_{\perp} for $d \leq 10$ kÅ and for H_{\parallel} over the entire thickness range. However, the technique might also prove useful in the measurement of normal resistivities of thin foils where contacts are difficult or impossible to attach. With reasonable frequencies (100 cps to 10 kcps) for foils of 0.1-mil thickness, resistivities in the range 10^{-10} to 10^{-8} Ω cm can be determined with relative ease.